

Article

Genome-Wide Identification of the NHX Gene Family in *Punica granatum* L. and Their Expressional Patterns under Salt Stress

Jianmei Dong^{1,2}, Cuiyu Liu^{1,2}, Yuying Wang^{1,2}, Yujie Zhao^{1,2}, Dapeng Ge^{1,2} and Zhaohe Yuan^{1,2,*}

¹ Co-Innovation Center for Sustainable Forestry in Southern China, Nanjing Forestry University, Nanjing 210037, China; djm@njfu.edu.cn (J.D.); cuiyu88@gmail.com (C.L.); wangyuying@njfu.edu.cn (Y.W.); z1184985369@njfu.edu.cn (Y.Z.); gedapeng@njfu.edu.cn (D.G.)

² College of Forestry, Nanjing Forestry University, Nanjing 210037, China

* Correspondence: zhyuan88@hotmail.com

Abstract: Most cultivated lands are suffering from soil salinization, which is a global problem affecting agricultural development and economy. High NaCl concentrations in the soil result in the accumulation of toxic Cl⁻ and Na⁺ in plants. Na⁺/H⁺ antiporter (NHX) can regulate Na⁺ compartmentalization or efflux to reduce Na⁺ toxicity. This study aims to identify the NHX genes in pomegranate (*Punica granatum* L.) from the genome sequences and investigate their expression patterns under different concentrations of NaCl stress. In this study, we used the sequences of *PgNHXs* to analyze the physicochemical properties, phylogenetic evolution, conserved motifs, gene structures, *cis*-acting elements, protein tertiary structure and expression pattern. A total of 10 *PgNHX* genes were identified, and divided into three clades. Conserved motifs and gene structures showed that most of them had an amiloride-binding site (FFI/LY/FLLPPI), except for the members of clade III. There were multiple *cis*-acting elements involved in abiotic stress in *PgNHX* genes. Additionally, protein-protein interaction network analysis suggested that *PgNHXs* might play crucial roles in keeping a balance of Na⁺ in cells. The qRT-PCR analysis suggested that *PgNHXs* had tissue-specific expressional patterns under salt stress. Overall, our findings indicated that the *PgNHXs* could play significant roles in response to salt stress. The theoretical foundation was established in the present study for the further functional characterization of the NHX gene family in pomegranate.

Keywords: pomegranate; NHX gene family; salt stress; phylogenetic analysis; expression pattern



Citation: Dong, J.; Liu, C.; Wang, Y.; Zhao, Y.; Ge, D.; Yuan, Z. Genome-Wide Identification of the NHX Gene Family in *Punica granatum* L. and Their Expressional Patterns under Salt Stress. *Agronomy* **2021**, *11*, 264. <https://doi.org/10.3390/agronomy11020264>

Academic Editor: Søren Kjærsgaard Rasmussen
Received: 28 December 2020
Accepted: 28 January 2021
Published: 30 January 2021

Publisher's Note: MDPI stays neutral with regard to jurisdictional claims in published maps and institutional affiliations.



Copyright: © 2021 by the authors. Licensee MDPI, Basel, Switzerland. This article is an open access article distributed under the terms and conditions of the Creative Commons Attribution (CC BY) license (<https://creativecommons.org/licenses/by/4.0/>).

1. Introduction

Soil salinization has become one of the harmful factors for the loss of cultivated land. Most of the world's arable lands are suffering from soil salinization, which is a global problem affecting agricultural development and economy [1]. The total areas of global saline-alkali soil have even reached 1.0×10^8 hm² since in the 1980s, which are still expanding [2]. Plant growth and development are affected by salt stress due to the destruction of osmotic balance and water deficiency [3–5].

When plants suffer from salt stress, Na⁺ will enter the cells through the non-selective ion channels and high-affinity K⁺ transporter-1 (HKT1) protein [6]. A high concentration of salt will disturb the balance of ions. Therefore, maintaining or reconstructing ionic equilibrium is essential for plants, the key of which is to reduce the concentration of Na⁺ in the cytoplasm. Plants relieve the harmful effects of excessive Na⁺ by separating Na⁺ into the vacuoles or removing Na⁺ from the cells [7]. The capacity of Na⁺ compartmentalization and exclusion was mainly relying on the activities of ion transporters [8]. Ion transporters mainly consist of HKT1 and Na⁺/H⁺ antiporter (NHX) in plants under salt stress [9,10]. The former can regulate the long-distance transport of Na⁺, while the latter can control the compartmentalization or efflux of Na⁺.

Na⁺/H⁺ antiporter is belongs to the NHX gene family and is widely distributed in all organisms [11]. Na⁺/H⁺ antiporter could be recognized as homodimers in the cell

membrane, with 10–12 transmembrane regions at the N terminus. The highly conservative regions of TM6 and TM7 could transport Na^+ and H^+ [12]. *NHX* genes play significant roles in osmotic regulation, stoma regulation and flower development [13,14]. The salt-tolerant effect of *NHX* genes has been highlighted, with the production of salt-tolerant transgenic plants. The *NHX* genes have also been identified in many plants, but the number of members is varied. For instance, there are eight *NHX* genes in *Arabidopsis thaliana* (L.) Heynh [15], six in grapevine (*Vitis vinifera* L.) [16], five in sugar beet (*Beta vulgaris*) [17], seven in sorghum (*Sorghum bicolor* (L.) Moench) [18], 10 in soybean (*Glycine max* (L.) Merr.) [6], and 25 in cotton (*Gossypium barbadense* L.) [19]. Among the eight *NHX* genes in *Arabidopsis*, *AtNHX1*, *AtNHX2*, *AtNHX3*, and *AtNHX4* were located on the vacuolar membrane; *AtNHX5*, and *AtNHX6* were located on the endosomal; and *AtNHX7* (*AtSOS1*) and *AtNHX8* were located on the plasma membrane. They were divided into Vacu-clade, Endo-clade, and Plas-clade, respectively, according to their subcellular location [15,17]. *AtNHX1*, *AtNHX2*, *AtNHX3*, *AtNHX4*, *AtNHX5*, and *AtNHX6* could participate in vesicle transport and cell expansion activities and regulate pH and K^+ . *AtNHX7* endowed plants with salt tolerance by the SOS (Salt overly sensitivity) pathway. The SOS pathway includes *SOS1*, *SOS2* (serine/threonine protein kinase), and *SOS3* (calcineurin), and the *SOS2-SOS3* compound could regulate *SOS1* to remove Na^+ from the cell [20,21]. *AtNHX8* located on the plasma membrane, was also considered a Li^+/H^+ antiporter [22,23].

Pomegranate (*Punica granatum* L.) belongs to the Lythraceae family, with significant ecological, cultural and economic values [24–26]. Pomegranate with moderate salt tolerance is predominantly grown in arid and semi-arid regions [27,28]. Bhantana et al. [29] pointed out that pomegranate could be listed as a model crop for perennial deciduous fruit trees, and it is of a great significance for investigation into the response mechanism to abiotic stress. Our previous study found that Na^+ accumulation in pomegranate tissues was closely associated with its salt tolerance under NaCl stress [27,28]. Thus, studying the *NHX* genes and their expression patterns in pomegranate tissues will contribute to revealing the mechanisms of Na^+ uptake and transport. However, there are few studies based on the Na^+/H^+ antiporter, despite many kinds of research focused on the pomegranate salt tolerance [30–32].

In the present study, the *NHX* gene family in pomegranate was identified based on the genome sequences (ASM220158v1) [33]. Additionally, various characteristics of *PgNHX* genes were analyzed, including their conserved domains, gene structures, phylogenetic relationship, *cis*-acting elements, protein-protein interaction network, and qRT-PCR analysis. Our results could reveal the roles of *PgNHXs* in response to salt stress, and our study aimed to provide a valuable reference for the further functional verification of the *NHX* genes in pomegranate.

2. Materials and Methods

2.1. Identification and Sequence Analysis of *PgNHXs*

We downloaded the protein sequences of the *NHX* genes in *Arabidopsis* from the Arabidopsis Information Resource (TAIR) database (<http://www.arabidopsis.org/>) [34]. We then used the BLASTP to search for candidate *PgNHXs* from the pomegranate genome (set the cut-off at E-value of $\leq 1 \times 10^{-10}$) [35]. The conserved protein domains of putative *PgNHXs* were confirmed using the Conserved Domain Database (CDD) (<https://www.ncbi.nlm.nih.gov/cdd>) [36] and simple modular architecture research tool (SMART) (<http://smart.embl-heidelberg.de>) [37].

The physicochemical properties of *PgNHX* proteins were predicted by ExpASY online tools (<http://expasy.org/protparam/>) [38], including amino acid residue lengths, molecular weight (MW), and isoelectric point (pI). Signal peptide information on the *PgNHX* proteins was predicted by SignalP v4.1 Server (<http://www.cbs.dtu.dk/services/SignalP-4.1/>) [39]. Transmembrane helices (TMHs) in *NHX* protein sequences were predicted by using TMHMM Server v2.0 (<http://www.cbs.dtu.dk/services/TMHMM-2.0/>). Subcellu-

lar localization in the NHX protein sequences was predicted by Cell-Ploc v2.0 package (<http://www.csbio.sjtu.edu.cn/bioinf/plant-multi/>) [40].

2.2. Phylogenetic Analysis

Multiple sequence alignment was conducted by Clustal W (v2.1, Dublin, Ireland) using the NHX protein sequences from eight angiosperms, including two monocots *Oryza sativa* L. (Os, four sequences, 485–545 aa) and *Zea mays* L. (Zm, six sequences, 538–545 aa), and six core eudicots *Arabidopsis thaliana* (L.) Heynh. (At, eight sequences, 503–1146 aa), *Citrus sinensis* (L.) Osbeck (Cs, six sequences, 439–1148 aa), *Eucalyptus grandis* Hill ex Maiden (Eg, six sequences, 525–1145 aa), *Punica granatum* L. (Pg), *Populus euphratica* Oliv. (Pe, seven sequences, 423–1145 aa), and *Vitis vinifera* L. (Vv, six sequences, 524–541 aa). All accession numbers and sequences of NHX proteins were presented in Supplementary File S1. The result of multiple sequence alignment of NHXs was visualized by Jalview [41]. A whole phylogenetic tree was constructed by MEGA (v5.0) [42] with the following settings: the neighbor-joining (NJ) method, 1000 bootstrap replicates, the Jones-Taylor-Thornton (JTT) model, and pairwise deletion. The EvolView (<http://www.evolgenius.info/evolview/#login>) [43] was then used to visualize it.

2.3. Motif Identification and Gene Structure Analysis

Multiple Expectation Maximization for Motif Elicitation (MEME) (<http://meme-suite.org/tools/meme>) [44] could be used to acquire the conserved motifs of NHX proteins from eight species. Parameter settings that influence the query execution result were set as followed: the maximum number of motifs 10, and the optimum motif width ≥ 6 and ≤ 50 .

The coding sequence (CDS) was aligned with the corresponding pomegranate genomic DNA sequences to generate the intron/exons of PgNHX genes and analyze gene structures. Gene structures could be demonstrated using the TBtools (v1.075, Guangzhou, China) [45].

2.4. Protein Tertiary Structure and Protein Interaction Network Analysis

To investigate the tertiary structure of PgNHX proteins, I-TASSER (<https://zhanglab.ccmb.med.umich.edu/I-TASSER/>) [46] was used to predict the structure of 10 PgNHX proteins. The Local Meta-Threading Server (LOMETS) was a multiple threading approach that could be used to search structure templates from the Protein Data Bank (PDB). Then we constructed a table about structural dependent modelling parameters for the PgNHX proteins.

We analyzed the interaction network of PgNHX proteins using a model plant *Arabidopsis* on the String protein interaction database (<http://string-db.org/>) [47].

2.5. Cis-Acting Elements Located in NHX Gene Promoters

Based on the pomegranate genome, 1500 bp upstream sequences of NHX genes were acquired. PlantCARE (<http://bioinformatics.psb.ugent.be/webtools/plantcare/html/>) [48] was used to analyze them, with the default parameter.

2.6. Plant Material, Treatment, and qRT-PCR Analysis

One-year-old ‘Taishanhong’ pomegranate cuttings were grown in pots (32 cm × 25 cm) filled with a mixture substrate (turf and perlite 1:1), which were put in a phytotron of the Nanjing Forestry University (Nanjing, China) with a photoperiod of 14 h lighting/10 h darkness, temperatures of 28 °C (lighting)/22 °C (darkness), and 60% humidity. Three completely randomized blocks were designed in the present study with a total of 24 pots. Every eight pots were designed as a block, and there were two pots per biological replicate, each plot containing one plant. The mixed solution containing 0 (control), 100, 200, or 300 mM NaCl (Guangzhou Chemical Reagent Factory, Guangzhou, China) supplemented with half-strength Hoagland’s nutrient solution (Shanghai yuanye Bio-Technology Co., Ltd, Shanghai, China) was watered in each pot every 6 days, respectively. Moisture was

maintained by placing a saucer under each container. All samples of leaves and roots were collected separately after 18 days of treatments.

Total RNA was extracted from pomegranate leaves and roots using a Trizol Total RNA Kit (Bio Teke, Wuxi, China). After that, the extracted RNA was used as a template for reverse transcription to obtain cDNA using the PrimeScript™ RT reagent kit with gDNA Eraser (TaKaRa, Beijing, China). As shown in Table 1, there were sequences of primers used for qRT-PCR. The PCRs were performed on 7500 Real-Time PCR System (Applied Biosystems, Foster City, CA, USA) with a TB Green Premix Ex Taq™ II Kit (TaKaRa, Beijing, China). The thermal cycler was set as follows: (a) 95 °C for 34 s, 95 °C for 5 s, 60 °C for 34 s for 40 cycles, and at the second step of each cycle, fluorescence was obtained; (b) a dissolution curve was acquired as followed: 95 °C for 15 s, 60 °C for 60 s and 95 °C for 15 s. Three biological replicates were used for this study. The method of $2^{-\Delta\Delta CT}$ [49] was adopted to represent relative expression levels of the *PgNHX* genes. The logarithm (base 2) was taken for the relative expression values, and represented by TBtools with heatmap.

Table 1. The sequences of primers used for qRT-PCR.

No.	Gene Name	Gene ID	Forward Primer Sequence (5'-3')	Reverse Primer Sequence (5'-3')
1	<i>PgNHX01</i>	<i>CDL15_Pgr020251</i>	AGTTGCTCGGAACCTTTCTC	CAGCATCATGAGAGCGACTT
2	<i>PgNHX02</i>	<i>CDL15_Pgr020284</i>	TGGGACATACTCATCTGCGA	CCATGCTGGTCCTATGCTTT
3	<i>PgNHX03</i>	<i>CDL15_Pgr013571</i>	TGTGATTGAACCTCCAGCAG	CTGTCCTTGCAATCGTCTCA
4	<i>PgNHX04</i>	<i>CDL15_Pgr008437</i>	AGCTCGTCAGTGATAGTCCA	TGATCTGTTGCTTCCAGTCG
5	<i>PgNHX05</i>	<i>CDL15_Pgr018608</i>	CTGATTATGGTGGGAAGGGC	TCCTGACCTCGTGAAGTATGAT
6	<i>PgNHX06</i>	<i>CDL15_Pgr016272</i>	CTTCCATCGTGACTGGACTG	GAGAGCCGTGATTGATTCTG
7	<i>PgNHX07</i>	<i>CDL15_Pgr004028</i>	GTTAGGCCTGCACATCGTAA	ACTATAGCTGTGGTAGCCGT
8	<i>PgNHX08</i>	<i>CDL15_Pgr019015</i>	TACTTTCGGCAACGGATTCA	GGCATCATTACGACTCCTT
9	<i>PgNHX09</i>	<i>CDL15_Pgr012091</i>	TGTGCTCGATGCTCCATGTT	AGTCACGGCTTGCGTTCATA
10	<i>PgNHX10</i>	<i>CDL15_Pgr021015</i>	CACAGGCACTCTGTTTGTCT	CCAATATTCGCCTCTTCGCT
11	<i>PgACTIN</i>	<i>CDL15_Pgr015157</i>	AGTCCTCTTCCAGCCATCTC	ACTGAGCACAATGTTTCCA

3. Results

3.1. Identification and Sequence Analysis of *PgNHXs*

In total, 10 putative *PgNHX* genes were identified from the pomegranate genome. All the *PgNHX* genes were renamed according to the order of protein id. The physical and chemical properties showed that the CDS length of 10 *PgNHXs* ranged from 1419 bp (*PgNHX09*) to 3582 bp (*PgNHX10*) (Table 2). The amino acid lengths were exhibited from 472 aa (*PgNHX09*) to 1193 aa (*PgNHX10*). The molecular weight ranged from 52.60 kDa (*PgNHX09*) to 132.31 kDa (*PgNHX10*). The predicted pI ranged from 5.45 (*PgNHX07*) to 9.32 (*PgNHX09*). The *PgNHX04* and *PgNHX07* were unstable proteins with high protein instability index (45.44 and 43.64 respectively), while other *PgNHX* proteins were stable. The grand average of hydropathy (GRAVY) value varied from 0.103 (*PgNHX10*) to 0.577 (*PgNHX09*), suggesting that all *PgNHX* proteins were hydrophobins. None of the *PgNHX* were secretory proteins and none had any signal peptide (Figure S1). In total, 10 *PgNHXs* were typical transmembrane transporters. *PgNHX04* contained 12 transmembrane helices. *PgNHX01* and *PgNHX09* contained 11 transmembrane helices. The other seven proteins had ten transmembrane helices (Figure S2). The prediction of subcellular localization showed that most of these *PgNHX* proteins might located in the vacuoles, while *PgNHX03* could be found in the vacuoles and on the cell membranes, and *PgNHX10* was only located on the cell membranes.

3.2. Phylogenetic Analysis

NHX proteins with full-length sequences from pomegranate and the other seven species were used to construct a phylogenetic tree to analyze the phylogenetic relationship of *PgNHX* genes (Figure 1). According to the phylogenetic tree, all the NHX proteins were divided into three obvious clades: clades I, II and III, with strong support

(Bootstrap = 100%). Clade I was the largest clade, including 38 NHXs (7 PgNHXs). Clade II was the smallest clade including 7 NHXs (PgNHX07). Clade III had 8 NHXs, including PgNHX03 and PgNHX10.

Table 2. The identification and sequence analysis of the Na⁺/H⁺ antiporter (NHX) gene family in pomegranate.

Gene Name	Protein ID	CDS (bp)	Length (aa)	MW (kDa)	pI	Instability Index	GRAVY	TMHs	Subcellular Localization
PgNHX01	OWM62957.1	1644	547	60.4	8.67	36.23	0.574	11	Vacuole
PgNHX02	OWM62990.1	1659	552	61.0	7.74	34.04	0.545	10	Vacuole
PgNHX03	OWM66354.1	2826	941	103.8	5.59	35.77	0.425	10	Cell membrane; Vacuole
PgNHX04	OWM74126.1	1632	543	60.6	9.21	45.44	0.479	12	Vacuole
PgNHX05	OWM78039.1	1617	538	59.5	9.32	35.22	0.571	10	Vacuole
PgNHX06	OWM78548.1	1626	541	60.4	8.17	39.49	0.476	10	Vacuole
PgNHX07	OWM83599.1	1647	548	60.0	5.45	43.64	0.401	10	Vacuole
PgNHX08	OWM85391.1	1653	550	60.3	8.32	36.53	0.546	10	Vacuole
PgNHX09	OWM85841.1	1419	472	52.6	6.94	35.40	0.577	11	Vacuole
PgNHX10	OWM90710.1	3582	1193	132.3	6.58	39.11	0.103	10	Cell membrane

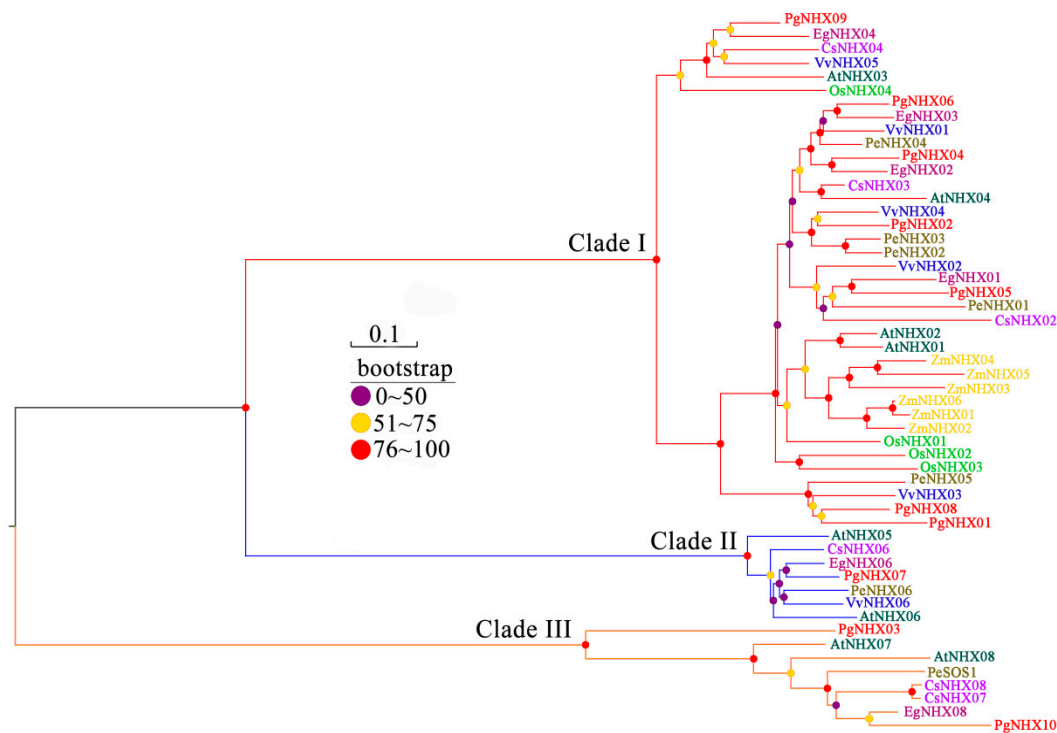


Figure 1. The phylogenetic tree of the NHX gene family, and sequences from *Arabidopsis thaliana* (L.) Heynh. (At), *Citrus sinensis* (L.) Osbeck (Cs), *Eucalyptus grandis* Hill ex Maiden (Eg), *Oryza sativa* L. (Os), *Populus euphratica* Oliv. (Pe), *Punica granatum* L. (Pg), *Vitis vinifera* L. (Vv) and *Zea mays* L. (Zm). Various branch colors indicate different clades. The species are presented by various font colors. The values of bootstrap are presented by three coloured pots.

3.3. Motif Identification and Gene Structure of PgNHXs

A combined figure, including a phylogenetic tree, multiple sequence alignment, conserved motifs, and sequence logo showed characteristics of the NHX gene family (Figure 2). The conservative motif distribution of PgNHX proteins were consistent with the phylogenetic tree. Hence, PgNHXs in the same clade presented similar conserved motif compositions. Here, motifs 1–10 were mainly presented in clade I. However, motif 3 were absent from clades II and III, and motif 4 was lost in clade II. Interestingly, the amiloride-binding site (FFI/LY/FLLPPI), a typical feature of NHX protein, was presented in motif 1. We could see that the site was presented in most NHX proteins, but absent from clade III. There were differences in the amiloride-binding site concerning the composition. For instance, most of

the proteins were FFIYLLPPI in clade I, while FFLFLLPPI in clade II. Residue IY or LF at this position could be known to be related to its sensitivity to amiloride [15]. Differentiation of sensitivity to amiloride indicated for NHX in different tissues is most likely involved in the structure of the protein, such as an accessory regulatory co-factor [50]. Those results might reveal that evolutionary patterns exist in this amiloride-binding site.

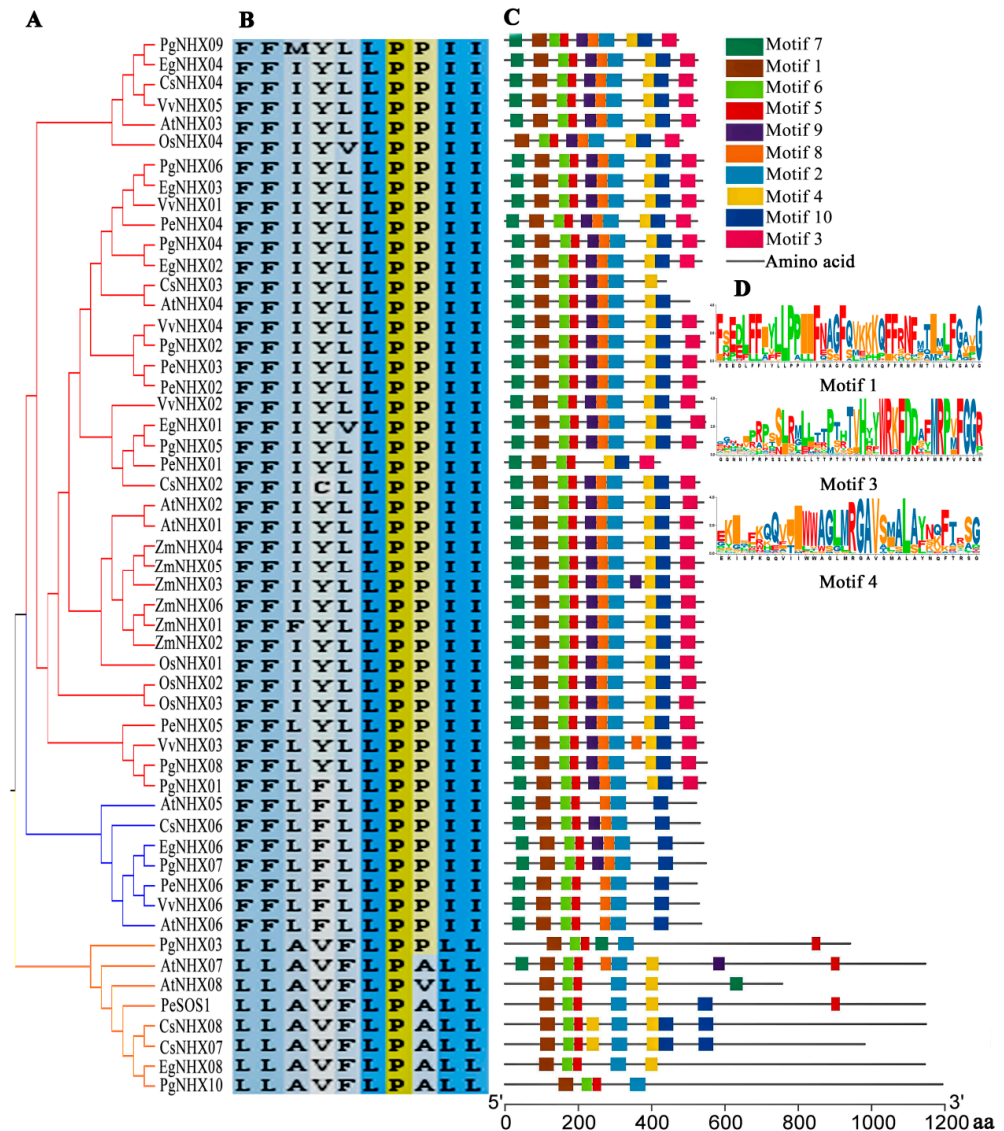


Figure 2. Phylogenetic tree, alignments and conserved motifs of the NHX gene family. (A) The phylogenetic tree of 53 NHX proteins as shown in Figure 1. (B) Multiple sequence alignment of the amiloride-binding site. (C) Conserved motifs in the PgNHX proteins. Different colored boxes represented different conserved motifs. (D) Sequence logo of motifs 1, 3 and 4.

Members from the same clade had similar gene structures, including the exon/intron number, intron phase, and exon length (Figure 3). The results of the gene structure showed that *PgNHX09*, *PgNHX07*, *PgNHX03*, and *PgNHX10* contained 13, 22, 21, and 23 exons, respectively, while other 6 *PgNHX* genes all had 14 exons. Overall, there was a unique and relatively conservative intron-exon arrangement.

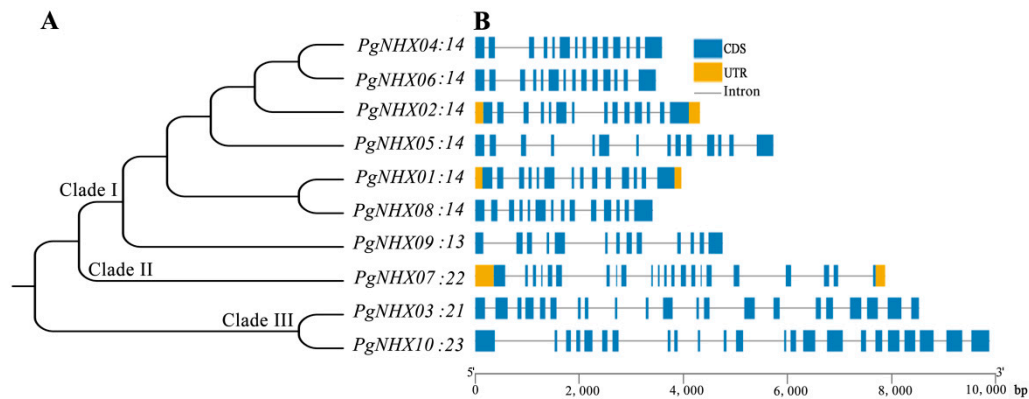


Figure 3. Phylogenetic tree, and gene structures of the PgNHX genes. (A) The phylogenetic tree of 10 PgNHX proteins. (B) Gene structures of the PgNHX genes. Blue boxes represent exons. Yellow boxes represent UTR.

3.4. Protein Tertiary Structure and Protein Interaction Network Analysis

All the NHX proteins in pomegranate were modeled by I-TASSER to understand their functional mechanism. Based on the ideal structural templates and crystal structures from PDB, tertiary structures of PgNHX protein were obtained (Figure 4). The confidence of constructed models evaluated by C-score, showed that its value generally ranged from -5 to 2 , and that the more reliable model had a higher value. In this study, the ten predicted NHX protein models in pomegranate with a high credibility, C-score varied from -1.92 (PgNHX09) to -0.11 (PgNHX10) (Table 3). Most proteins shared the same PDB hit 4cz8A, indicating that their tertiary structures were similar.

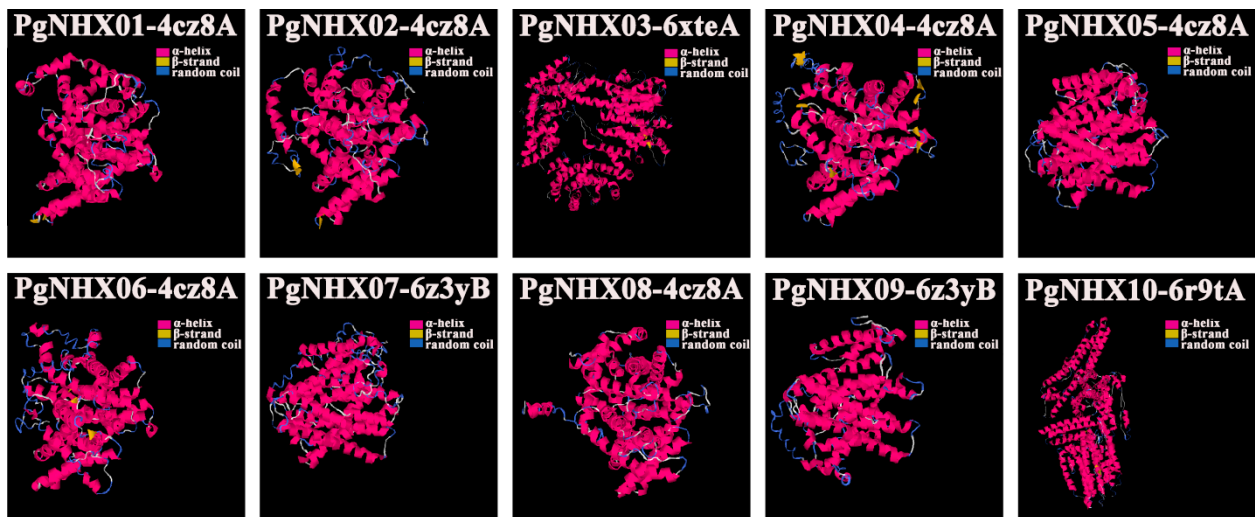


Figure 4. Tertiary structure of PgNHX proteins. The models of proteins were obtained by the online server I-TASSER. The α -helix, β -strand, and random coil are marked by red, yellow and blue, respectively. The parameters of the best PDB structure for PgNHXs are listed in Table 3.

To further explore the potential function, signal transduction and metabolic pathways of the PgNHX members, the protein-protein interaction network was constructed with the online tool String (Figure 5). All of them were on the protein-protein interaction network, and they shared the same putatively interactive proteins, including AVP1 (AT1G15690.1), HKT1 (AT4G10310.1), SOS2 (AT5G35410.1) and SOS3 (AT5G24270.2). AVP1 was involved in the regulation of apoplastic pH and auxin transport. HKT1 could play a significant role in Na^+ recirculation to roots from shoots. SOS2 and SOS3 were involved in the regulatory pathway of salt stress by controlling intracellular Na^+ and Ca^{2+} homeostasis, and directly

interacted with SOS1 (PgNHX03 and PgNHX10), NHX1 (PgNHX01 and PgNHX08), and NHX2 (PgNHX02, PgNHX04, PgNHX05 and PgNHX06). Additionally, the interaction between SOS1 and RCD1 (AT1G32230.1), might respond to high salt or oxidative stress. All PgNHX proteins worked together to respond to salt stress.

Table 3. Structural dependent modeling parameters for the PgNHX proteins.

Protein	C-Score	TM-Score	RMSD (Å)	Best Identified Structure Analogs in PDB				
				PDB Hit	TM-Score ^a	RMSD ^a	IDEN ^a	Cov
PgNHX01	−1.69	0.51 ± 0.15	11.5 ± 4.5	4cz8A	0.707	1.06	0.209	0.717
PgNHX02	−1.21	0.56 ± 0.15	10.4 ± 4.6	4cz8A	0.701	1.08	0.227	0.710
PgNHX03	−0.66	0.63 ± 0.14	10.3 ± 4.6	6xteA	0.925	0.96	0.089	0.932
PgNHX04	−1.50	0.53 ± 0.15	11.0 ± 4.6	4cz8A	0.702	1.50	0.210	0.720
PgNHX05	−1.67	0.51 ± 0.15	11.5 ± 4.5	4cz8A	0.697	1.93	0.204	0.729
PgNHX06	−1.80	0.50 ± 0.15	11.8 ± 4.5	4cz8A	0.702	1.51	0.223	0.723
PgNHX07	−1.48	0.53 ± 0.15	11.0 ± 4.6	6z3yB	0.690	1.31	0.402	0.704
PgNHX08	−0.81	0.61 ± 0.14	9.4 ± 4.6	4cz8A	0.702	1.17	0.212	0.713
PgNHX09	−1.92	0.48 ± 0.15	11.8 ± 4.5	6z3yB	0.742	1.38	0.301	0.761
PgNHX10	−0.11	0.70 ± 0.12	9.6 ± 4.6	6r9tA	0.986	0.87	0.105	0.991

Note: C-score ranged from −5 to 2, which signifies the confidence of each model. A higher value suggests a model with a higher confidence and vice-versa. TM-score and RMSD are evaluated derived from the C-score value and the protein length following the correlation observed between these qualities. The TM-score^a represents a measure of global structural similarity between query and template protein. RMSD^a represents the RMSD between residues that are structurally aligned by TM-align. IDEN^a represents identity of the percentage sequence in the structurally aligned region. Cov is coverage, representing the coverage of the alignment by TM-align, and its value is equal to the number of structurally aligned residues divided by length of the query protein.

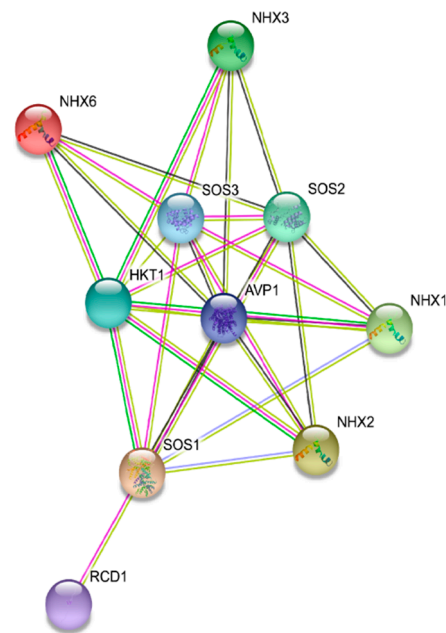


Figure 5. Protein-protein interaction network of PgNHX protein was analyzed by the Tool String. Network nodes represent proteins. Colored nodes represent query proteins and first shell of interactors. Empty nodes indicate proteins of unknown 3D structure. Filled nodes indicate that some 3D structure is known or predicted.

3.5. Cis-Acting Elements Located in Promoters of PgNHXs

We submitted upstream 1500 bp sequences in the promoter region to PlantCARE to obtain *cis*-acting elements. The results showed that 20 *cis*-elements involved in abiotic stress were found, including LTR, O2-site, ABRE, G-Box, CAAT-box, TGA-element, GARE-

motif, CGTCA-motif, GATA-motif, MBS, MRE, Sp1, P-box, TATC-box, Box 4, TCA-element, TCCC-motif, TGACG-motif, and AuxRR-core (Figure 6 and Table S1).

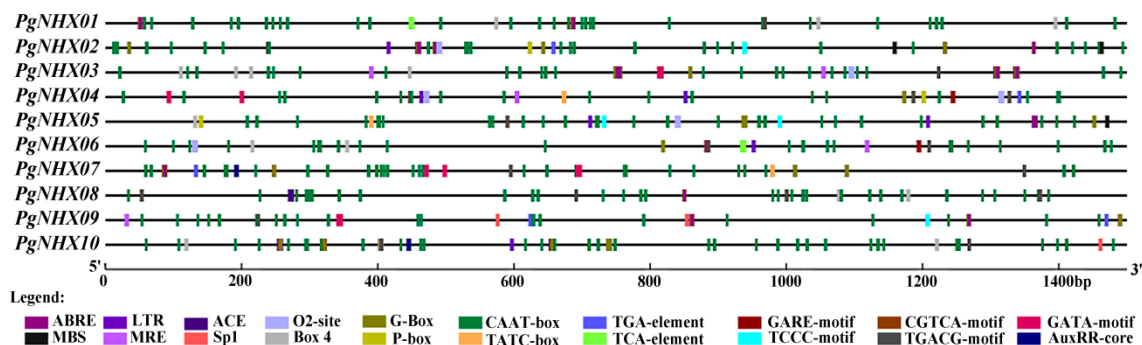


Figure 6. Cis-acting elements analysis of *PgNHX* genes. Note: ABRE was involved in the abscisic acid responsiveness; LTR involved in low-temperature responsiveness; ACE, MRE, Sp1, Box 4, G-Box, GATA-motif, and TCCC-motif were involved in light responsiveness; O2-site was involved in zein metabolism regulation; CAAT-box was involved in promoter and enhancer regions; TGA-element and AuxRR-core were involved in auxin-responsiveness; GARE-motif, P-box and TATC-box involved in gibberellin-responsiveness; CGTCA-motif and TGACG-motif were involved in the MeJA-responsiveness; MBS was involved in drought-inducibility; TCA was involved in salicylic acid responsiveness.

Most of the members contained ABA-responsive element ABRE, except *PgNHX04*. Half of the *PgNHX* genes contained the low-temperature stress response element LTR. *PgNHX* genes all contained two or more elements related to light responsiveness, including ACE, MRE, Sp1, Box 4, G-Box, GATA-motif, and TCCC-motif. 60% of the *PgNHX* genes contained elements of the GARE-motif, P-box and TATC-box and were involved in gibberellin response. All of the members of *PgNHX* genes contained MeJA responsive elements, CGTCA-motif and TGACG-motif. Only *PgNHX02* and *PgNHX05* contained the drought-inducibility element MBS. Only *PgNHX01* and *PgNHX06* contained the salicylic acid responsive element TCA. A total of 20% and 40% of *PgNHX* genes contained the auxin response element AuxRR-core and TGA-element. Above all, *PgNHX* genes might be related to the process of photosynthetic, hormone and adversity stress, and regulation of growth and development.

3.6. qRT-PCR Analysis of *PgNHXs* under Salt Stress

The results of the qRT-PCR analysis of *PgNHX* genes indicated that the expression patterns were tissue-specific under different NaCl treatments (Figure 7 and Table S2). Interestingly, the relative expression levels of all *PgNHX* genes in leaves were up-regulated, while most of *PgNHXs* were down-regulated or not changed in roots. At a low salinity level (100 mM NaCl), the relative expression levels in leaves were up-regulated, compared with the control (0 mM NaCl). The up-regulated expression of *PgNHX10* was almost 9-fold higher than that found in control plants. However, most of the *PgNHX* genes were the down-regulation in roots compared with control, especially *PgNHX01*. Under moderate salt stress (200 mM NaCl), the relative expression levels were increased continuously in leaves, except *PgNHX02* and *PgNHX08*. Meanwhile, *PgNHX02* and *PgNHX09* were up-regulated in roots compared with control. When subjected to severe salt stress (300 mM NaCl), the relative expression level still increased in leaves, and the expression level of *PgNHX04* in roots was higher than other treatments.

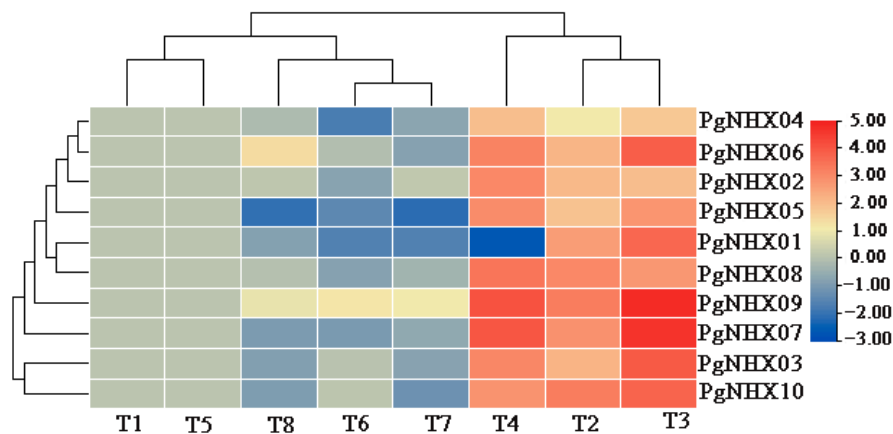


Figure 7. The relative expression levels of the PgNHX genes in leaves and roots under different NaCl treatments. T1, T2, T3, T4 represented the different treatments of 0, 100, 200, 300 mM NaCl in leaves, respectively. T5, T6, T7, T8 represented the different treatments of 0, 100, 200, 300 mM NaCl in roots, respectively.

4. Discussion

The *NHX* genes, coding for the Na^+/H^+ antiporter, belong to the CPA1 family. The Na^+/H^+ antiporter plays critical roles in the steady state of K^+ and pH, leaf development and responses to salt stress [13,14,51]. In the present study, we identified 10 *NHX* genes in pomegranate. PgNHX proteins all contained Na^+/H^+ exchanger domains, which were relatively conservative in the evolution.

According to the phylogenetic tree, all genes were divided into three clades. Among them, PgNHX01, PgNHX02, PgNHX04, PgNHX05, PgNHX06, PgNHX08, PgNHX09 and AtNHX01, AtNHX02, AtNHX03, AtNHX04 of the *Arabidopsis* were on the same branch of clade I. PgNHX07, AtNHX05 and AtNHX06 were on the same branch of clade II. PgNHX03, PgNHX10, AtNHX07 and AtNHX08 were on the same branch of clade III. Members of the same branch in the evolutionary tree might have similar biological functions. The evolutionary relationship was highly consistent with the subcellular location classification of *G.max*, *Brachypodium distachyon* (L.) Beauv., *Populus trichocarpa* Torr. & Gray ex Brayshaw and *Beta vulgaris* L. [17,52,53] As mentioned above, the *NHX* members of *Arabidopsis* were divided into three clades, according to its subcellular location: vacuolar membrane, endosomal and plasma membrane [15]. However, subcellular locations of PgNHX proteins were not consistent with *Arabidopsis*. Most of the PgNHX proteins were located in the vacuoles, while there were fewer on the cell membranes. Accordingly, this might indicate that the NaCl resistant mechanism of pomegranate was chiefly through the regionalization of Na^+ into vacuoles.

In pomegranate, clade I had fewer exons (13–14) than other two clades (21–23). The results were in line with the *NHX* proteins in sugar beet, soybean, and poplar [6,17,52]. Our result showed clearly that their gene structures were highly conserved. Additionally, the same clade had similar motif compositions, indicating that the gene structures of the *NHX* gene family were relatively conserved during evolution. The binding site of amiloride (FFI/LY/FLLPPI) is one of the typical characteristics of *NHX* proteins. *NHX* is highly sensitive to amiloride, and could be completely inhibited due to the high affinity of its specific amino acid residue to amiloride. Na^+ and amiloride could have the same functional binding site, according to amiloride, which was a competitive inhibitor of *NHX* mediating Na^+ transport [54,55]. In this study, the binding site of amiloride was found in most members, but missing in three members, including PgNHX03, PgNHX09 and PgNHX10. Similar amiloride-binding sites were observed in *V.vinifera*, *A.thaliana*, *P.trichocarpa* and *S.bicolor* [11,18,52]. This finding implied that the motif (FFI/LY/FLLPPI) on the transmembrane region of PgNHX is sensitive to the Na^+ of the substrate.

There were many *cis*-acting elements involved in hormone or abiotic stress response in the promoter region of the *PgNHX* genes. For example, most of the *PgNHX* genes had elements related to abscisic acid (ABA) regulation, low temperature, light, gibberellins, etc. These results might indicate that *PgNHX* genes participated in the growth and development of pomegranate through different hormone regulation pathways, abiotic stress response, and other physiological processes.

The protein-protein interaction network showed that the *PgNHXs* played a crucial role in salt-stress resistance. In the present study, we found that all *PgNHX* proteins shared the same putatively interactive protein AVP1, HKT1, SOS2 and SOS3. All of these putatively interacted proteins play essential roles in response to abiotic stress. Overexpression of the *AVP1* can increase the plant's tolerance to salt in *Arabidopsis* [56]. Romero-Aranda et al. [57] pointed out that HKT1 can improve salt tolerance by extracting Na^+ from the xylem of different tissues and organs. SOS2 can encode a protein kinase to alleviate salt stress in *Arabidopsis* [58]. SOS3 is a Ca^{2+} sensor, which can escort SOS2 and SOS1 to promote Na^+ efflux from the cells [18]. As shown in the summarized diagram, salt tolerance regulation is a multi-way regulation network (Figure 8). It is highly consistent with previous findings [58,59]. The increases in the transcription level of H^+ -ATPase, result in improving tolerance to salinity [60]. Moreover, we can also regulate the amount of K^+ by AKT1 to reduce salt damage [59]. It is well known that many plants tend to adapt to high salinity environments by maintaining a high K^+/Na^+ ratio. Notably, AKT1 plays important roles in K^+ uptake, maintenance and restoration of K^+ homeostasis under salt stress. The overexpression of AKT1 in transgenic *Arabidopsis* also indicates that AKT1 could enhance the salt resistance [61,62]. As explained above, the response processes of plant growth, development, biotic and abiotic stresses are closely related. Thus, they may have similar regulatory functions, and simultaneously induce expression during stress.

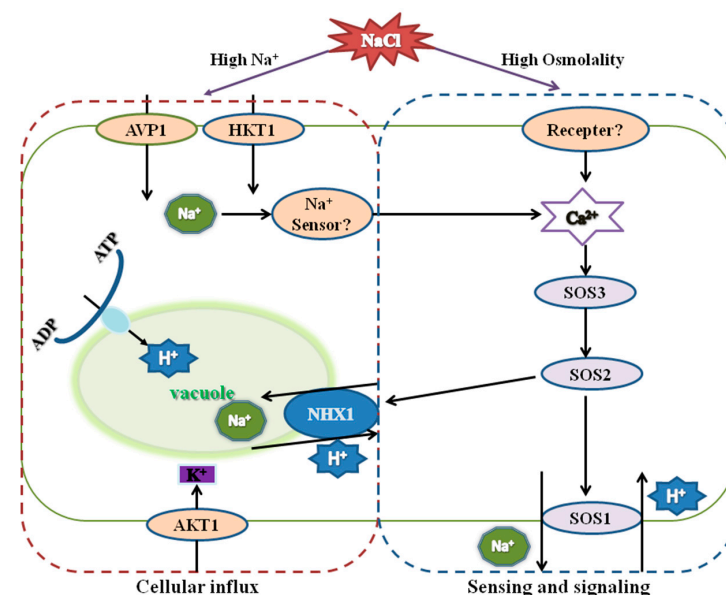


Figure 8. Cell signaling pathways that regulate activities of ion transporters to maintain K^+/Na^+ homeostasis under salt stress.

The results of qRT-PCR suggested that the relative expression levels of *PgNHXs* had tissue-specific expressional patterns in pomegranate under salt stress, and the expression levels in leaves were higher than roots. Such results might be due to the stimulation of *PgNHXs* with the increasing of NaCl concentration, Na^+ in leaf transfers from cytoplasm to vacuole, which were timely and effective, resulting in reducing ion toxicity [63]. Most genes showed adverse regulatory effects in roots, except *PgNHX06*. Under low and moderate salt stress, as the Na^+ accumulated, the relative expression levels in leaves

of pomegranate increased as well. Thus, Na⁺ could be up-taken or sequestered in the vacuoles of leaves. At a high salinity level, some *PgNHX* genes still had higher expression levels. However, at the same time, *PgNHX01* could not compartmentalize excessive Na⁺ in leaves so that expression level was drastically reduced in leaves. The results of tissue-specific expressional patterns of *NHX* were similar to Quintero et al. [64] and Wu et al. [65], and Na⁺ accumulation resulted in up-regulation in leaves rather than roots. Thus, the *PgNHX* genes might perform the different functions in pomegranate roots and leaves. *PgNHXs* might alleviate the harmful effects of Na⁺ via sequestering the excessive Na⁺ into vacuoles of leaves and reducing the Na⁺ accumulation in roots.

5. Conclusions

In the present study, 10 *PgNHX* genes were identified, and the same clade had similar motif compositions and gene structures. The tissue-specific expressional patterns were displayed in *PgNHX* genes, with relatively low expression levels in roots and high expression levels in leaves under different concentrations of NaCl stress. The *PgNHX* genes were related to the uptake and transport of Na⁺ in pomegranate. Overall, our results could provide a reference for further research on the stress response of *PgNHX* and the functional verification of *PgNHX*.

Supplementary Materials: The following are available online at <https://www.mdpi.com/2073-4395/11/2/264/s1>, Table S1: *Cis*-elements of 10 *PgNHXs*, Table S2: The relative expression levels of 10 *PgNHXs*, File S1: All protein sequences for tree, Figure S1: Signal peptide prediction of 10 *PgNHX* proteins, Figure S2: Transmembrane helices of 10 *PgNHX* proteins.

Author Contributions: Conceptualization, J.D. and Z.Y.; methodology, Y.W. and D.G.; software, Y.W.; formal analysis, J.D.; investigation, J.D. and C.L.; writing—original draft preparation, J.D.; writing—review and editing, J.D., C.L., Y.W., Y.Z., D.G. and Z.Y.; supervision, C.L., Y.W., Y.Z. and Z.Y.; funding acquisition, Z.Y. All authors have read and agreed to the published version of the manuscript.

Funding: This research was funded jointly by the Tibet Autonomous Region Natural Science Foundation [XZ201019ZRG-153], the Initiative Project for Talents of Nanjing Forestry University [GXL2014070, GXL2018032], the Priority Academic Program Development of Jiangsu High Education Institutions [PAPD], and the Natural Science Foundation of Jiangsu Province [BK20180768].

Conflicts of Interest: The authors declare no conflict of interest.

References

- Zhu, J.K. Plant salt tolerance. *Trends Plant Sci.* **2001**, *6*, 66–71. [[CrossRef](#)]
- Kovda, V.A. Loss of productive land due to salinization. *Ambio* **1983**, *12*, 91–93. [[CrossRef](#)]
- Xiong, L.M.; Zhu, J.K. Molecular and genetic aspects of plant responses to osmotic stress. *Plant Cell Environ.* **2002**, *25*, 131–139. [[CrossRef](#)] [[PubMed](#)]
- Tester, M.; Davenport, R. Na⁺ tolerance and Na⁺ transport in higher plants. *Ann. Bot.* **2003**, *91*, 503–527. [[CrossRef](#)] [[PubMed](#)]
- Abdul Qados, A.M.S. Effect of salt stress on plant growth and metabolism of bean plant *Vicia faba* L. *J. Saudi Soc. Agric. Sci.* **2011**, *10*, 7–15. [[CrossRef](#)]
- Chen, H.T.; Chen, X.; Wu, B.-Y.; Yuan, X.X.; Zhang, H.M.; Cui, X.Y.; Liu, X.Q. Whole-genome identification and expression analysis of K⁺ efflux antiporter (*KEA*) and Na⁺/H⁺ antiporter (*NHX*) families under abiotic stress in soybean. *J. Integr. Agric.* **2015**, *14*, 1171–1183. [[CrossRef](#)]
- Fukuda, A.; Nakamura, A.; Hara, N.; Toki, S.; Tanaka, Y. Molecular and functional analyses of rice *NHX*-type Na⁺/H⁺ antiporter genes. *Planta* **2010**, *233*, 175–188. [[CrossRef](#)]
- Farooq, M.; Hussain, M.; Wakeel, A.; Siddique, K.H.M. Salt stress in maize: Effects, resistance mechanisms, and management. A review. *Agron. Sustain. Dev.* **2015**, *35*, 461–481. [[CrossRef](#)]
- Rubio, F.; Gassmann, W.; Schroeder, J.I. Sodium-driven potassium uptake by the plant potassium transporter *HKT1* and mutations conferring salt tolerance. *Science* **1995**, *270*, 1660–1663. [[CrossRef](#)]
- Apse, M.P.; Aharon, G.S.; Snedden, W.A.; Blumwald, E. Salt tolerance conferred by overexpression of a vacuolar Na⁺/H⁺ antiport in *Arabidopsis*. *Science* **1999**, *285*, 1256–1258. [[CrossRef](#)]
- Ayadi, M.; Ben Ayed, R.; Mzid, R.; Aifa, S.; Hanana, M. Computational approach for structural feature determination of grapevine *NHX* antiporters. *BioMed Res. Int.* **2019**, *2019*, 1–13. [[CrossRef](#)] [[PubMed](#)]

12. Dibrov, P.; Fliegel, L. Comparative molecular analysis of Na⁺/H⁺ exchangers: A unified model for Na⁺/H⁺ antiport? *FEBS Lett.* **1998**, *424*, 1–5. [[CrossRef](#)]
13. Qiu, Q.S. Plant and yeast NHX antiporters: Roles in membrane trafficking. *J. Integr. Plant Biol.* **2012**, *54*, 66–72. [[CrossRef](#)] [[PubMed](#)]
14. Bassil, E.; Zhang, S.Q.; Gong, H.J.; Tajima, H.; Blumwald, E. Cation specificity of vacuolar NHX-type cation/H⁺ antiporters. *Plant Physiol.* **2019**, *179*, 616–629. [[CrossRef](#)] [[PubMed](#)]
15. Brett, C.L.; Donowitz, M.; Rao, R. Evolutionary origins of eukaryotic sodium/proton exchangers. *Am. J. Physiol. Cell Physiol.* **2005**, *288*, C223–C239. [[CrossRef](#)] [[PubMed](#)]
16. Ayadi, M.; Martins, V.; Ben Ayed, R.; Jbir, R.; Feki, M.; Mzid, R.; Géros, H.; Aifa, S.; Hanana, M. Genome wide identification, molecular characterization, and gene expression analyses of grapevine NHX antiporters suggest their involvement in growth, ripening, seed dormancy, and stress response. *Biochem. Genet.* **2020**, *58*, 102–128. [[CrossRef](#)] [[PubMed](#)]
17. Wu, G.Q.; Wang, J.L.; Li, S.J. Genome-wide Identification of Na⁺/H⁺ antiporter (NHX) genes in sugar beet (*Beta vulgaris* L.) and their regulated expression under salt stress. *Genes* **2019**, *10*, 401. [[CrossRef](#)]
18. Kumari, H.; Kumar, S.; Ramesh, K.; Palakolanu, S.R.; Marka, N.; Prakash, A.; Shah, T.; Henderson, A.; Srivastava, R.; Rajashekar, G.; et al. Genome-wide identification and analysis of arabidopsis sodium proton antiporter (NHX) and human sodium proton exchanger (NHE) homologs in *Sorghum bicolor*. *Genes* **2018**, *9*, 236. [[CrossRef](#)]
19. Akram, U.; Song, Y.; Liang, C.; Abid, M.; Askari, M.; Myat, A.; Abbas, M.; Malik, W.; Ali, Z.; Guo, S.; et al. Genome-wide characterization and expression analysis of NHX gene family under salinity stress in *Gossypium barbadense* and Its comparison with *Gossypium hirsutum*. *Genes* **2020**, *11*, 803. [[CrossRef](#)]
20. Qiu, Q.S.; Guo, Y.; Dietrich, M.A.; Schumaker, K.S.; Zhu, J.K. Regulation of SOS1, a plasma membrane Na⁺/H⁺ exchanger in *Arabidopsis thaliana*, by SOS2 and SOS3. *Proc. Natl. Acad. Sci. USA* **2002**, *99*, 8436–8441. [[CrossRef](#)]
21. Quintero, F.J.; Ohta, M.; Shi, H.Z.; Zhu, J.K.; Pardo, J.M. Reconstitution in yeast of the *Arabidopsis* SOS signaling pathway for Na⁺ homeostasis. *Proc. Natl. Acad. Sci. USA* **2002**, *99*, 9061–9066. [[CrossRef](#)] [[PubMed](#)]
22. Wang, M.; Zheng, Q.S.; Shen, Q.R.; Guo, S.W. The critical role of potassium in plant stress response. *Int. J. Mol. Sci.* **2013**, *14*, 7370–7390. [[CrossRef](#)] [[PubMed](#)]
23. Meng, K.B.; Wu, Y.X. Footprints of divergent evolution in two Na⁺/H⁺ type antiporter gene families (NHX and SOS1) in the genus *Populus*. *Tree Physiol.* **2018**, *38*, 813–824. [[CrossRef](#)] [[PubMed](#)]
24. Yuan, Z.H.; Yin, Y.L.; Qu, J.L.; Zhu, L.Q.; Li, Y. Population genetic diversity in chinese pomegranate (*Punica granatum* L.) cultivars revealed by fluorescent-AFLP markers. *J. Genet. Genom.* **2017**, *34*, 1061–1071. [[CrossRef](#)]
25. Fahmy, H.; Hegazi, N.; El-Shamy, S.; Farag, M.A. Pomegranate juice as a functional food: A comprehensive review of its polyphenols, therapeutic merits, and recent patents. *Food Funct.* **2020**, *11*, 1–27. [[CrossRef](#)]
26. Tozzi, F.; Legua, P.; Martínez-Nicolás, J.J.; Núez-Gómez, D.; Melgarejo, P. Morphological and nutraceutical characterization of six pomegranate cultivars of global commercial interest. *Sci. Hortic.* **2020**, *272*, 1–9. [[CrossRef](#)]
27. Liu, C.Y.; Zhao, X.Q.; Yan, J.X.; Yuan, Z.H.; Gu, M.M. Effects of salt stress on growth, photosynthesis, and mineral nutrients of 18 pomegranate (*Punica granatum*) cultivars. *Agronomy* **2019**, *10*, 27. [[CrossRef](#)]
28. Liu, C.Y.; Zhao, Y.J.; Zhao, X.Q.; Wang, J.P.; Gu, M.M.; Yuan, Z.H. Transcriptomic profiling of pomegranate provides insights into salt tolerance. *Agronomy* **2020**, *10*, 44. [[CrossRef](#)]
29. Bhandana, P.; Lazarovitch, N. Evapotranspiration, crop coefficient and growth of two young pomegranate (*Punica granatum* L.) varieties under salt stress. *Agric. Water Manag.* **2010**, *97*, 715–722. [[CrossRef](#)]
30. Cui, J.Q.; Hua, Y.P.; Zhou, T.; Liu, Y.; Huang, J.Y.; Yue, C.P. Global landscapes of the Na⁺/H⁺ antiporter (NHX) family members uncover their potential roles in regulating the rapeseed resistance to salt stress. *Int. J. Mol. Sci.* **2020**, *21*, 3429. [[CrossRef](#)]
31. Li, W.H.; Du, J.; Feng, H.M.; Wu, Q.; Xu, G.H.; Shabala, S.; Yu, L. Function of NHX-type transporters in improving rice tolerance to aluminum stress and soil acidity. *Planta* **2020**, *251*, 71. [[CrossRef](#)] [[PubMed](#)]
32. Long, L.; Zhao, J.R.; Guo, D.D.; Ma, X.N.; Gao, W. Identification of NHXs in *Gossypium* species and the positive role of GhNHX1 in salt tolerance. *BMC Plant Biol.* **2020**, *20*, 147. [[CrossRef](#)] [[PubMed](#)]
33. Qin, G.H.; Xu, C.Y.; Ming, R.; Tang, H.B.; Guyot, R.; Kramer, E.M.; Hu, Y.D.; Yi, X.K. The pomegranate (*Punica granatum* L.) genome and the genomics of punicalagin biosynthesis. *Plant J.* **2017**, *91*, 1108–1128. [[CrossRef](#)] [[PubMed](#)]
34. Lamesch, P.; Berardini, T.Z.; Li, D.H.; Swarbreck, D.; Wilks, C.; Sasidharan, R. The Arabidopsis Information Resource (TAIR): Improved gene annotation and new tools. *Nucleic Acids Res.* **2012**, *40*, D1201–D1210. [[CrossRef](#)]
35. Zhang, T.; Liu, C.; Huang, X.; Zhang, H.; Yuan, Z. Land-plant phylogenomic and pomegranate transcriptomic analyses reveal an evolutionary scenario of CYP75 genes subsequent to whole genome duplications. *J. Plant Biol.* **2019**, *62*, 48–60. [[CrossRef](#)]
36. Marchler-Bauer, A.; Lu, S.; Anderson, J.B.; Chitsaz, F.; Derbyshire, M.K.; DeWeese-Scott, C.; Fong, J.H. CDD: A conserved domain database for the functional annotation of proteins. *Nucleic Acids Res.* **2011**, *39*, 225–229. [[CrossRef](#)]
37. Schultz, J.; Milpetz, F.; Bork, P.; Ponting, C.P. SMART, a simple modular architecture research tool: Identification of signaling domains. *Proc. Natl. Acad. Sci. USA* **1998**, *95*, 5857–5864. [[CrossRef](#)]
38. Gasteiger, E.; Hoogland, C.; Gattiker, A.; Duvaud, S.E.; Wilkins, M.R.; Appel, R.D.; Bairoch, A. *Protein Identification and Analysis Tools on the ExpASY Server*; Humana Press: Totowa, NJ, USA, 2005. [[CrossRef](#)]
39. Petersen, T.N.; Brunak, S.; Heijne, G.V.; Nielsen, H. SignalP 4.0: Discriminating signal peptides from transmembrane regions. *Nat. Methods* **2011**, *8*, 785–786. [[CrossRef](#)]

40. Chou, K.C.; Shen, H.B. Plant-mPLOC: A top-down strategy to augment the power for predicting plant protein subcellular localization. *PLoS ONE* **2010**, *5*, e11335. [[CrossRef](#)]
41. Michele, C.; James, C.; Stephen, M.S.; Geoffrey, J.B. The Jalview Java alignment editor. *Bioinformatics* **2004**, *20*, 426–427. [[CrossRef](#)]
42. Tamura, K.; Peterson, D.; Peterson, N.; Stecher, G.; Nei, M.; Kumar, S. MEGA5: Molecular evolutionary genetics analysis using maximum likelihood, evolutionary distance, and maximum parsimony methods. *Mol. Biol. Evol.* **2011**, *28*, 2731–2739. [[CrossRef](#)] [[PubMed](#)]
43. Subramanian, B.; Gao, S.H.; Lercher, M.J.; Hu, S.N.; Chen, W.H. Evolview v3: A webserver for visualization, annotation, and management of phylogenetic trees. *Nucleic Acids Res.* **2019**, *47*, W270–W275. [[CrossRef](#)] [[PubMed](#)]
44. Bailey, T.L.; Boden, M.; Buske, F.A.; Frith, M.; Grant, C.E.; Clementi, L.; Ren, J.Y.; Li, W.W.; Noble, W.S. MEME SUITE: Tools for motif discovery and searching. *Nucleic Acids Res.* **2009**, *37*, W202–W208. [[CrossRef](#)] [[PubMed](#)]
45. Chen, C.J.; Xia, R.; Chen, H.; He, Y.H. TBtools, a Toolkit for Biologists integrating various HTS-data handling tools with a user-friendly interface. *BioRxiv* **2018**, 289660. [[CrossRef](#)]
46. Yang, J.; Zhang, Y. I-TASSER Server: New development for protein structure and function predictions. *Nucleic Acids Res.* **2015**, *43*, W174–W181. [[CrossRef](#)]
47. Szklarczyk, D.; Gable, A.L.; Lyon, D.; Junge, A.; Wyder, S.; Huerta-Cepas, J.; Simonovic, M.; Doncheva, N.T.; Morris, J.H.; Bork, P. STRING v11: Protein-protein association networks with increased coverage, supporting functional discovery in genome-wide experimental datasets. *Nucleic Acids Res.* **2018**, *47*, D607–D613. [[CrossRef](#)]
48. Lescot, M.; Déhais, P.; Thijs, G.; Marchal, K.; Moreau, Y.; Van de Peer, Y.; Rouzé, P.; Rombauts, S. PlantCARE, a database of plant cis-acting regulatory elements and a portal to tools for in silico analysis of promoter sequences. *Nucleic Acids Res.* **2002**, *30*, 325–327. [[CrossRef](#)]
49. Livak, K.J.; Schmittgen, T.D. Analysis of relative gene expression data using realtime quantitative PCR and the $2^{-\Delta\Delta CT}$ method. *Methods* **2001**, *25*, 402–408. [[CrossRef](#)]
50. Yun, C.H.C.; Little, P.J.; Nath, S.K.; Levine, S.A.; Pouyssegur, J. Leu143 in the putative fourth membrane spanning domain is critical for amiloride inhibition of an epithelial Na^+/H^+ exchanger isoform (NHE-2). *Biochem. Biophys. Res. Commun.* **1993**, *193*, 532–539. [[CrossRef](#)]
51. Li, N.N.; Wang, X.; Ma, B.J.; Du, C.; Zheng, L.L.; Wang, Y.C. Expression of a Na^+/H^+ antiporter *RtNHX1* from a recretohalophyte *Reaumuria trigyna* improved salt tolerance of transgenic *Arabidopsis thaliana*. *J. Plant Physiol.* **2017**, *218*, 109–120. [[CrossRef](#)]
52. Tian, F.X.; Chang, E.; Li, Y.; Sun, P.; Hu, J.J.; Zhang, J. Expression and integrated network analyses revealed functional divergence of *NHX*-type Na^+/H^+ exchanger genes in poplar. *Sci. Rep.* **2017**, *7*, 2607. [[CrossRef](#)] [[PubMed](#)]
53. Bassil, E.; Coku, A.; Blumwald, E. Cellular ion homeostasis: Emerging roles of intracellular *NHX* Na^+/H^+ antiporters in plant growth and development. *J. Exp. Bot.* **2012**, *63*, 5727–5740. [[CrossRef](#)] [[PubMed](#)]
54. Counillon, L.; Franchi, A.; Pouyssegur, J. A point mutation of the Na^+/H^+ exchanger gene (*NHE1*) and amplification of the mutated allele confer amiloride resistance upon chronic acidosis. *Proc. Natl. Acad. Sci. USA* **1993**, *90*, 4508–4512. [[CrossRef](#)] [[PubMed](#)]
55. Harris, C.; Fliegel, L. Amiloride and the Na^+/H^+ exchanger protein: Mechanism and significance of inhibition of the Na^+/H^+ exchanger (review). *Int. J. Mol. Med.* **1999**, *3*, 315–336. [[CrossRef](#)] [[PubMed](#)]
56. Gaxiola, R.A.; Li, J.L.; Undurraga, S.; Dang, L.M.; Fink, G.R. Drought- and salt-tolerant plants result from overexpression of the *AVP1* H^+ -pump. *Proc. Natl. Acad. Sci. USA* **2001**, *98*, 11444–11449. [[CrossRef](#)] [[PubMed](#)]
57. Romero-Aranda, M.R.; Fernández, P.G.; López-Tienda, J.R.; López-Díaz, M.R.; Espinosa, J.; Granum, E.; Traverso, J.Á.; Pineda, B.; Garcia-Sogo, B.; Moreno, V.; et al. Na^+ transporter *HKT1;2* reduces flower Na^+ content and considerably mitigates the decline in tomato fruit yields under saline conditions. *Plant Physiol. Biochem.* **2020**, *154*, 341–352. [[CrossRef](#)]
58. Wilkins, K.A.; Matthus, E.; Swarbreck, S.M.; Davies, J.M. Calcium-mediated abiotic stress signaling in roots. *Front. Plant Sci.* **2016**, *7*, 1296. [[CrossRef](#)]
59. Manik, S.M.N.; Shi, S.J.; Mao, J.J.; Dong, L.H.; Su, Y.L.; Wang, Q.; Liu, H. The calcium sensor *CBL-CIPK* is involved in plant's response to abiotic stresses. *Int. J. Genom.* **2015**, *2015*, 1–10. [[CrossRef](#)]
60. Bao, A.K.; Wang, S.M.; Wu, G.Q.; Xi, J.J.; Wang, C.M. Overexpression of the *Arabidopsis* H^+ -PPase enhanced resistance to salt and drought stress in transgenic alfalfa (*Medicago sativa* L.). *Plant Sci.* **2008**, *176*, 232–240. [[CrossRef](#)]
61. Chen, J.; Wang, W.H.; Wu, F.H.; He, E.M.; Zheng, H.L. Hydrogen sulfide enhances salt tolerance through nitric oxide-mediated maintenance of ion homeostasis in barley seedling roots. *Sci. Rep.* **2015**, *5*, 12516. [[CrossRef](#)]
62. Chen, Z.; Zhao, X.; Hu, Z.; Leng, P. Nitric oxide modulating ion balance in *Hylotelephium erythrostictum* roots subjected to NaCl stress based on the analysis of transcriptome, fluorescence, and ion fluxes. *Sci. Rep.* **2019**, *9*, 18137. [[CrossRef](#)] [[PubMed](#)]
63. Ape, M.P.; Sottosanto, J.B.; Blumwald, E. Vacuolar cation/ H^+ exchange, ion homeostasis, and leaf development are altered in a T-DNA insertional mutant of *AtNHX1*, the *Arabidopsis* vacuolar Na^+/H^+ antiporter. *Plant J.* **2003**, *36*, 229–239. [[CrossRef](#)] [[PubMed](#)]
64. Quintero, F.J.; Blatt, M.R.; Pardo, J.M. Functional conservation between yeast and plant endosomal Na^+/H^+ antiporters. *FEBS Lett.* **2000**, *471*, 224–228. [[CrossRef](#)]
65. Wu, C.A.; Yang, G.D.; Meng, Q.W.; Zheng, C.C. The cotton *GhNHX1* gene encoding a novel putative tonoplast Na^+/H^+ antiporter plays an important role in salt stress. *Plant Cell Physiol.* **2004**, *45*, 600–607. [[CrossRef](#)] [[PubMed](#)]